Leaflet No.

The Republic of the Union of Myanmar
Ministry of Natural Resources and Environmental Conservation
Forest Department

Revisiting Tethyan Evolution: Insights from the Early Carboniferous Magmatic Arc in Eastern Myanmar

San Win, Department of Geological Survey and Mineral Exploration
Qinglai Feng , China University of Geosciences, China
Ye Myint Swe[c], Myanmar Geoscience Society, Yangon, Myanmar
Tianyu Zhao, China University of Geosciences, China
Zhengqin Gan, Xiaomei Nie , China University of Geosciences, China
Aung Khaing, Consultant Geologist, Mining Association of Eastern Shan State, Myanmar.
Sai Naing Lin Aung, University of Yangon, Department of Geology, Myanmar

February, 2024

Table of Content

Revisiting Tethyan Evolution: Insights from the Early Carboniferous Magmatic Arc in Eastern Myanmar

San Win [a,b*], Qinglai Feng [a], Ye Myint Swe[c], Tianyu Zhao[a], Zhengqin Gan[a], Xiaomei Nie[a], Aung Khaing[d], Sai Naing Lin Aung[e]

[a] State Key Laboratory of Geological Processes and Mineral Resources, School of Earth Sciences, China University of Geosciences, Wuhan 430074, China.

[b] Department of Geological Survey and Mineral Exploration, Nay Pyi Taw, Myanmar.

[c] Myanmar Geoscience Society, Yangon, Myanmar.

[d] Consultant Geologist, Mining Association of Eastern Shan State, Myanmar.

[e] University of Yangon, Department of Geology, Myanmar.

Abstract

Eastern Myanmar is a crucial region linking SW Yunnan and northern Thailand, critical for enhancing our comprehension of Tethyan evolution. The abundant and well-preserved geological records in these regions provide an optimal setting for studying the tectonic evolution of Proto- and Paleo-Tethys. However, the precise location and evolution of the Tethyan suture zone in Eastern Myanmar remain obscure. This study focuses on the geochronological, geochemical, and zircon Lu-Hf isotopic analysis of plutonic rocks in the Tachileik area, including granite, diorite, and gabbroic rocks. In-situ zircon U-Pb dating of these plutonic rocks indicates an Early Carboniferous emplacement, with weighted mean ages approximating 353-355 Ma. The Tachileik granites exhibit characteristics typical of I-type granites, being high-K calc-alkaline, weakly peraluminous, and possessing low P_2O_5 content. These granites display positive zircon $\varepsilon_{Hf(t)}$ values (+4.5 to +7.4) and T_{DM2} ages ranging from 981 to 825 Ma, suggesting a juvenile mafic lower crust source. The Tachileik gabbros and diorites, classified under tholeiitic and calc-alkaline basalt series, display high Al_2O_3 and Mg# levels, along with low TiO_2 and K_2O contents. These intermediate-mafic rocks reveal enrichment in large ion lithophile elements (LILE) and depletion in high field strength elements (HFSE), resembling volcanic arc basalt with distinctly negative Nb and Ta anomalies. Both zircon Hf isotopic signatures and geochemical data suggest that the genesis of these intermediate-mafic rocks could be attributed to the partial melting of subduction-metasomatized lithospheric mantle within an arc-related setting, specifically within the spinel stability field. In summary, the Tachileik plutonic rocks originated within a subduction-related environment, corresponding to the subduction of the Proto-Tethys during the Early Carboniferous. This study provides persuasive evidence, indicating that the subduction of Proto-Tethys began in the early Carboniferous in eastern Shan State, Myanmar.

Keywords: Tethys; Early Carboniferous; Plutonic rocks; Subduction; Tachileik; Eastern Myanmar

1. Introduction

Southwest China (SW China) and Southeast Asia (SE Asia) serve as critical areas for understanding the evolution of the Tethyan realm, making them focal points for investigating Proto- and Paleo-Tethys evolution (Sengor et al., 1988; Metcalfe, 2013). Extensive research has identified the Changning-Menglian Belt in SW Yunnan and the Chiang Mai Belt in northern Thailand as significant regions, representing the sutures of the primary Paleo-Tethyan oceanic basin and the collisional boundary between the Sibumasu and Indochina-Yangtze blocks (Liu et al., 1991; Zhong, 1998; Feng, 2002; Metcalfe, 2011; Wang et al., 2017). Eastern Shan State of Myanmar is a crucial link between SW Yunnan and northern Thailand, providing essential insights into Tethyan evolution. However, conducting research in this Myanmar region presents formidable challenges due to security issues, inadequate transportation, dense vegetation, and extensive weathered granitic soil cover In past decade, the study on the Paleo-Tethys in this area has made good progress (Ridd et al., 2015; Gardiner et al., 2016; Barber et al., 2017; Mitchell, 2018; Hu et al., 2020; Cong et al., 2021), but the research about Proto-Tethys has not been reported. How to extend the Proto-Tethys orogenic belt southward in Yunnan is still a mystery (Nie et al., 2016; Zhao et al., 2017; Wei et al., 2020; Liu et al., 2021).

Recently, the Early Carboniferous magmatic rocks, such as gabbro, diorite, and granite, in the northern and western regions of Tachileik have been discovered. In this study, we present a comprehensive analysis encompassing petrological, geochronological, bulk-rock geochemical, and zircon Lu-Hf isotopic data on these rocks. We aim to research petrogenesis, tectonic setting, and their potential linkage with the Proto-Tethyan orogenic zone in SW Yunnan.

2. Regional Geology

In Southeast Asia, two significant continental blocks, the Indochina and Sibumasu blocks, play crucial roles in the region's geological evolution (Metcalfe, 2017). During the Devonian, the Indochina Block initiated from Gondwana due to the opening of Paleo-Tethys, while in the Late Carboniferous to Early Permian, the Sibumasu Block rifted away from Gondwana (Metcalfe, 2017). The Sibumasu Block includes Eastern Myanmar (Shan State), Northwest Thailand, Peninsular Burma and Thailand, western Malaya, Sumatra, and possibly extends northwards into SW China and Tibet (Metcalfe, 1984).

Tectonically, Eastern Myanmar can be categorized into three parts: the Sibumasu Block, the Mong Yang-Mong Ton Suture Zone, and the Indochina Block (Fig. 1). The Mong Yang-Mong Ton Suture Zone links to the Changning–Menglian Suture Zone in the north and the Chiang Mai Suture Zone in the south, marking the position of the primary Paleo-Tethys Ocean.

In Eastern Myanmar, the Indochina Block hosts two significant magmatic rock belts known as the Main Range and Eastern Provinces (Fig. 1). The Main Range Province comprises the Keng Tung granite and lower metamorphic rocks. The Keng Tung granite, predominantly S-type granites, dates back to the Late Triassic to the early Jurassic, ~ 200-227 million years ago (Sone & Matcalfe, 2008; Gardiner et al., 2016), and correlated with the Lincang granite in SW Yunnan. The lower metamorphic rocks are the equivalent of the Lancang Group in SW Yunnan, spanning from the Ediacaran to Silurian (Wei et al., 2022).

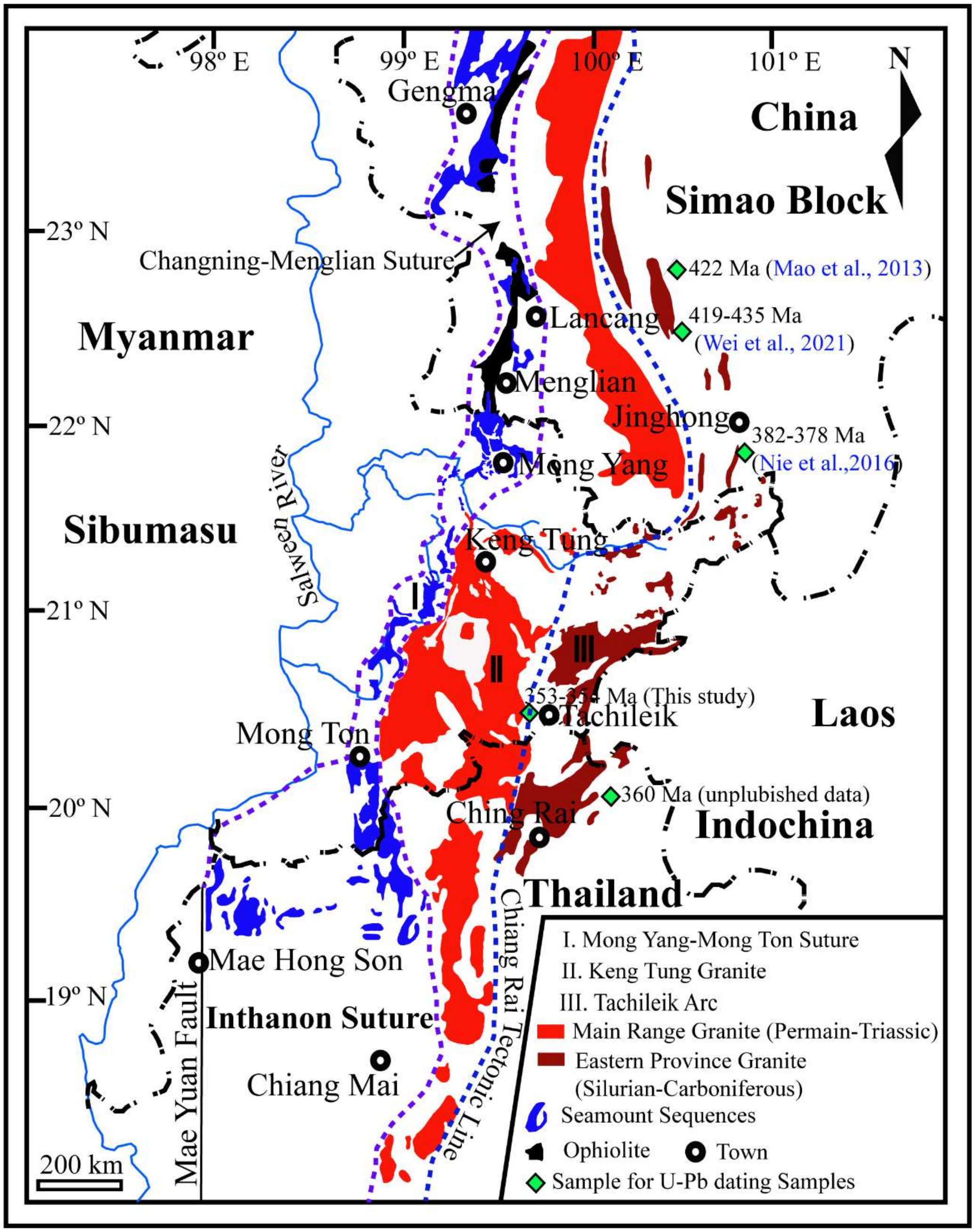

Figure 1: Tectonic units in Eastern Myanmar with adjacent Thailand and China (after Barber et al., 2017)

The Eastern Province, stated as the Tachileik Arc, comprises Precambrian-Cambrian metamorphic rocks, Carboniferous-Permian sedimentary strata, and magmatic rocks (Fig. 2). These magmatic rocks include Permian-Triassic hornblende biotite granite and granodiorite, diorite, gabbroic rocks, and andesite (Gardiner et al., 2016). They are classified as I-type granite and island arc volcanic rocks associated with the Sukhothai Arc, formed by the eastward subduction of Paleo-Tethys beneath the western margin of the Indochina block (Sone & Matcalfe, 2008).

Moreover, besides the Permian-Triassic magmatic rocks, recent research includes Early Carboniferous magmatic rocks, such as gabbro and granite, distributed in the north and west of the Tachileik area (Fig. 2).

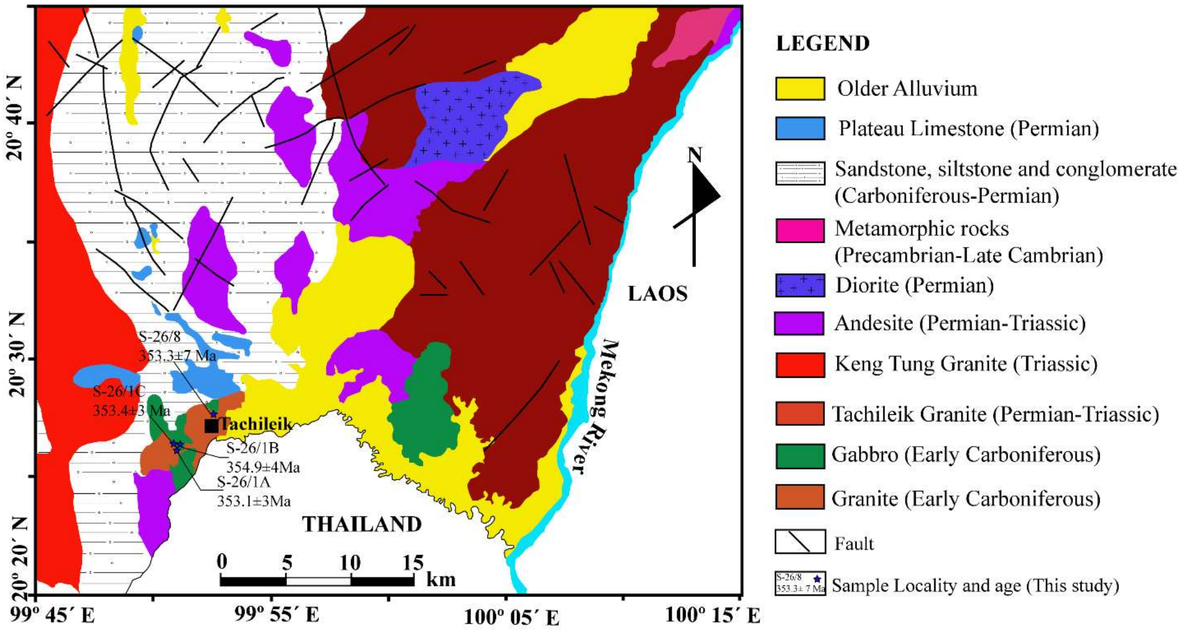

Figure 2: Geological map and sample location map of the study area (After Aung Min et al., 2016)

3. Studied Materials

The studied materials were collected from the Tachileik area, Eastern Shan State. Sample S-26/8 is taken from the outcrop located to the north of Tachileik (Fig. 2), and the rock is highly weathered. Therefore, it is only suitable for studying zircon chronology, but not suitable for thin section and geochemical study. Investigation site S-26/1, located to the west of Tachileik (Fig. 2), is the outcrop of a valley, and fresh rock outcrops appear intermittently along a stream. Their lithology is different in the outcrops, which may be structural fragments of different lithology. Three samples representing different lithologies were collected, including granite, diorite, and amphibole gabbro. The petrological characteristics of these three samples are as follows.

Sample S-26/1A is granite (Fig.3a and b) which is composed mainly of feldspar and quartz mosaic intergrown with the accessory constituents of biotite and chlorite. The feldspar consists mainly of perthite and plagioclase. The perthites are anhedral to subhedral crystals up to 5 mm, while the plagioclases are subhedral to euhedral crystals up to 4 mm in size. Most of the plagioclases show polysynthetic twinning and a few amounts of plagioclases show slightly zoned character. Some perthite crystals up to 0.5 cm in size are also found. All of the feldspars are turbid due to kaolinization and sericitization. Qurartz are observed as anhedral crystals up to 5 mm in size. Some micas show yellowish-brown to dark brown colored biotite, yellowish to green pleochroic color, and a few muscovites are colorless. Some biotite flakes are more or less altered to green chlorite. The opaque specks are observed as anhedral grains.

The sample S-26/1B diorite (Fig.3c and d) consists mainly of feldspar and hornblende with smaller amounts of opaque minerals. Almost all of the feldspars are polysynthetically twinned plagioclases and albites. They are subhedral to anhedral crystals up to 2 mm in size.

Some plagioclases partially alter to saussurite. The hornblende crystals show subhedral in shape and light brown to green pleochroic. Some hornblendes show simple twin, and some are altered to chlorites.

Thin section observation of the sample gabbro S-26/1C (Fig.3e and f) shows that the sample consists mainly of plagioclase feldspar, albite, amphibole and a few pyroxenes. Well twinned plagioclase feldspars show subhedral prismatic shape up to 5 mm long. The plagioclases are also altered to sericite and epidote. Anhedral crystals of augite are also detected. Some pyroxenes are partially or totally replaced by fibrous amphibole. Light green to green pleochroic colored hornblendes have been identified. The green-colored fibrous chlorite is also noted. Minor sphene and opaque minerals up to 1.5 mm in size are disseminated throughout the rock.

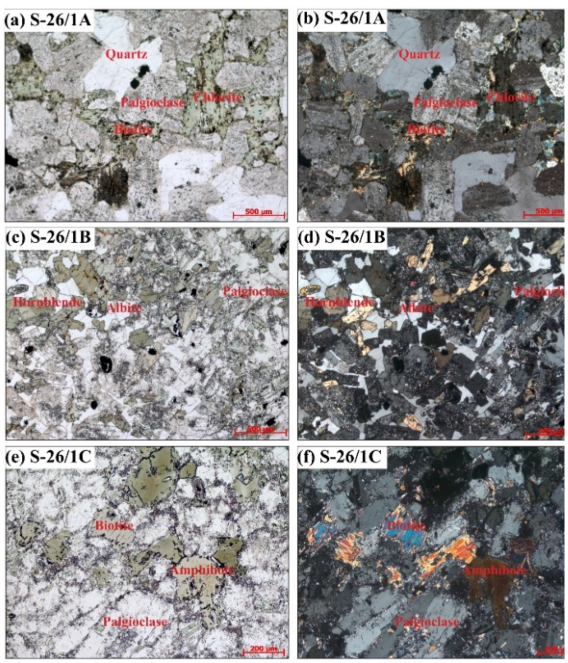

Figure 3: Photomicrographs of S-26/1A-Granite, S-26/1B-Diorite, and S-26/1C-Amphibole Gabbro, under plane-polarized light (left) and cross-polarized light (right).

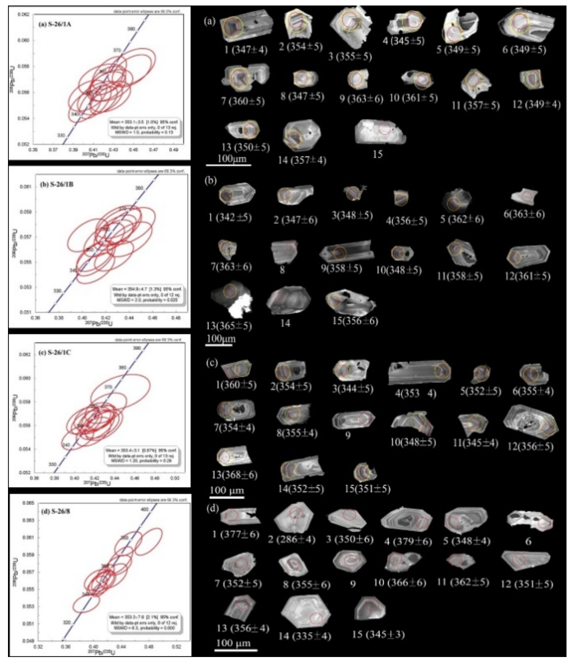

Figure 4: Cathodoluminescence images (CL) of the representative zircons and U-Pb Concordia diagrams of the plutonic rocks from the Tachileik area, (a) S-26/1A, (b) S-26/1B, (c) S-26/1C and (d) S-26/8.

Analytical Results

4.1 Zircon U-Pb ages

Four representative samples (S-26/1A, S-26/1B, S-26/1C, and S-26/8) were chosen for zircon U-Pb dating. Zircon grains extracted from these samples (Fig. 4) generally exhibit subhedral to euhedral morphology. Cathodoluminescence (CL) images reveal that these zircons typically have luminescent (Low U) cores with well-defined fine-scale oscillatory igneous zoning. The size of the zircon grains typically falls within the range of 30 to 160 µm in length and 50-80 µm in width.

The analytical results of a coherent group yielded weighted mean 206Pb/238U ages for the granite sample S-26/1A at 353.1±3 Ma (MSWD 1.4) (Fig. 4), the diorite sample S-26/1B at 354.9±4 Ma (MSWD 2.0) (Fig. 4), the amphibole gabbro sample S-26/1C at

353.4±3 Ma (MSWD 1.2) (Fig. 4), and the weathered granite sample S-26/8 at 353.3±7 Ma (MSWD 2.0) (Fig. 4). These results indicate that the samples from this study area yielded ages ranging approximately from 353.1 to 354.9 Ma, suggesting that the plutonic rocks were formed during the Early Carboniferous.

4.2 Zircon Lu-Hf isotopic data

Three samples (S-26/1A, S-26/1B, and S-26/1C) were chosen for Hf isotopic analyses based on the dated zircon samples.

The analysis of zircon dated at 353.1 Ma from granite sample S-26/1A revealed initial 176Hf/177Hf ratios ranging from 0.28510 to 0.282770, yielding εHf(t) values from -2.5 to +7.4. These values correspond to single-stage model ages (TDM1) of 1128-698 Ma and two-stage model ages (TDM2) of 1360-824 Ma. However, one sample showed a negative value of -2.5, significantly deviating from the other data (mean=6.2), thus interpretation is unreliable for discussion.

Zircons dated at 354.9 Ma from the diorite sample S-26/1B \yielded initial 176Hf/177Hf ratios ranging from 0.282251 to 0.282757, with εHf(t) values varying from -11 to 7.1. These values correspond to single-stage model ages (TDM1) of 1128-698 Ma and two-stage model ages (TDM2) of 1441-703 Ma. Similarly, one sample exhibited a negative value of -11, significantly deviating from the rest of the data (mean=5.4), and thus was considered invalid.

Zircons from the 353.4 Ma amphibole gabbro S-26/1C displayed initial 176Hf/177Hf ratios ranging from 0.282703 to 0.282768, with εHf(t) values ranging from 4.9 to 6.2. These values correspond to single-stage model ages (TDM1) of 802 -716 Ma and two-stage model ages (TDM2) of 959-839 Ma. The 176Lu/177Hf values are close to or less than 0.003, indicating no significant radiogenic Hf accumulation after the crystallization of these zircons. All analyzed spots exhibited positive zircon εHf(t) values ranging from +2.5 to +7.4 (Fig.5), suggesting that these rocks were primarily derived from the partial melting of juvenile crustal material.

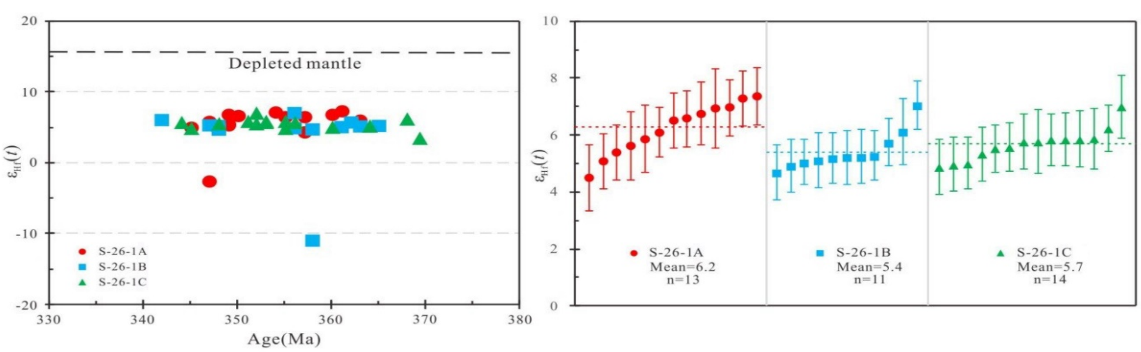

Figure 5: Plots of U-Pb ages (Ma) vs. ε_{Hf}(t)of in-situ zircon from Tachileik area, Eastern Shan State.

4.3 Geochemistry

All plutonic rock samples, including S-26/1A, S-26/1B, and S-26/1C, underwent comprehensive whole-rock major, trace, and rare earth element (REE) analyses. Examination of the QAP diagram (Fig. 6a; Streckeisen, 1967) and Na_2O+K_2O vs. SiO_2 plot (Fig.6b; Le Maitre, 1989) revealed that S-26/1A falls within the granite field, while the other two samples (S-26/1B and S-26/1C) fall into the diorite and gabbro fields, respectively (Fig.6b).

Furthermore, according to the Plag/Px/Hb diagram, sample S-26/1C, representing gabbroic rock, falls within the amphibole gabbro field (Fig.7).

The granite samples (S-26/1A) exhibit high SiO_2 (74.53 - 74.91 wt.%), Al_2O_3 (12.76-12.94 wt.%), and K_2O (4.65-4.68 wt.%), but low TiO_2 (0.19-0.20 wt.%), MgO (0.20–0.22 wt.%), Mg# (16.6–17.1), Cr (0.47–0.61 ppm), and V (5.23–5.86 ppm) contents. They display relatively enriched LREEs ($(La/Yb)_N$ = 9.9–10.7) and flat heavy rare-earth element (HREE) patterns ($(Gd/Yb)_N$=1.-1.4) (Fig. 8). Additionally, they exhibit moderate negative Eu anomalies with Eu/Eu* = 0.72–0.75 (Fig. 8a). The granites also demonstrate strong negative HFSEs (e.g., Nb, Ta, and Ti) and enrichment in LILEs (Rb and K), Th, and U. In the SiO_2 vs. K_2O diagram (Fig.9a; Rickwood, 1989), these samples align with the high-K calc-alkaline series. They belong to the weak peraluminous series with A/CNK values of 1.0 -1.1 (Fig.9b). The granite S-26/1A exhibits characteristics consistent with I-type granites, being weakly peraluminous with high K_2O/Na_2O (>1), low CaO (<0.64 wt.%) and MgO (<0.20 wt.%), and low Sr (91.1 ppm–94.7 ppm) and P_2O_5 (0.02 ppm-0.03 ppm).

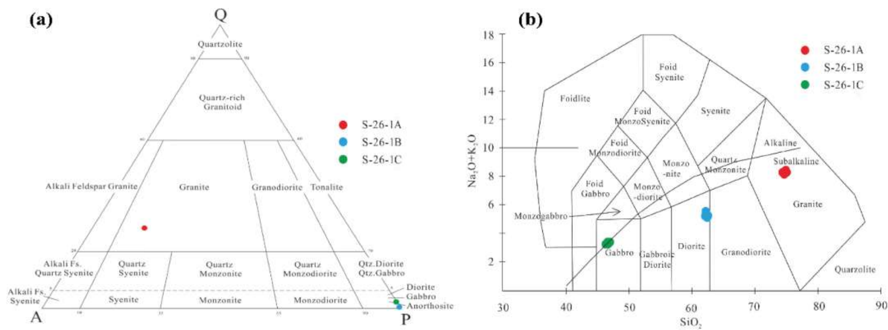

Figure 6: Whole-rock composition of the Plutonic rocks from Tachileik area, (a). QAP Modal classification (after Streckeisen, 1967), (b) Na_2O+K_2O Vs SiO_2 (after LeMaitre, 1989)

The diorite samples S-26/1B have low SiO_2 content ranging from 62.61 - 62.89 wt.%, K_2O (0.87-0.88 wt.%), and $K_2O + Na_2O$ (5.21–5.35 wt.%), but high concentrations of Al_2O_3 (15.51–15.56 wt.%), MgO (2.22–2.26 wt.%), and CaO (4.55–4.58 wt.%) (Table 1). They exhibit subalkaline and medium-K calc-alkaline character in the total alkali–silica (TAS) diagram (Fig. 7), and medium-K calc-alkaline character (Fig. 10a). The diorite are characterized by high Na_2O/K_2O ratios (4.9–5.0) and low A/CNK (0.93–0.95), indicating metaluminous compositions (Fig. 10b). They also display LREEs enrichment features ($(La/Yb)_N$ = 6.18-12.98) with weakly negative Eu anomalies (Eu/Eu* = 0.93–0.95) (Fig. 8a) and enrichment in LILEs (such as Rb, Ba, and K) and depletion in HFSE (Nb, Ta, Zr, Hf, and Ti), consistent with the geochemical characteristics of subduction-related magmas.

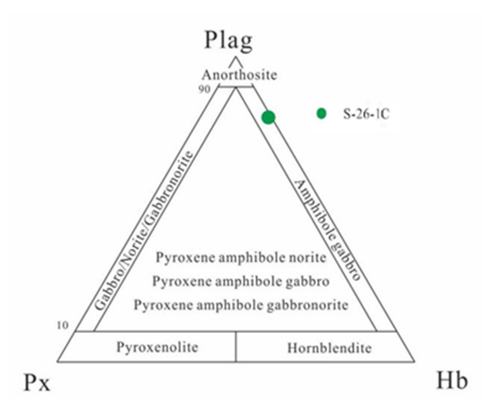

Figure 7: Plag-Px-Hb diagram for Sample-S-26/1C yields Amphibole gabbro.

The amphibole gabbro S-26/1C exhibits low SiO_2 (46.24-46.61 wt.%) and K_2O (0.49-0.50 wt.%) contents but high values of MgO (7.63–7.67 wt.%), Mg# (57.5–57.6), TFe_2O_3 (13.06–13.22 wt.%), Cr (84–85 ppm), and V (325–328 ppm). The sample S-26/1C belongs to the calc-alkaline series (Fig. 9a). These samples are dominantly metaluminous, as indicated by their low aluminum saturation index A/CNK (0.69-0.71, Fig. 9b). The amphibole gabbro is slightly enriched in LREE and shows relatively flat heavy rare-earth element (HREE) patterns, similar to Enriched Mid-Ocean Ridge Basalts (E-MORB) (Fig. 9a). They exhibit weak positive Eu anomalies with Eu/Eu* = 1.03–1.09 (Fig. 8a) and show enrichment in large ion lithophile elements (LILEs; e.g., Rb, Ba, and K) and depletion in high field-strength elements (HFSEs; e.g., Nb, Ta, and Ti) (Fig. 8b).

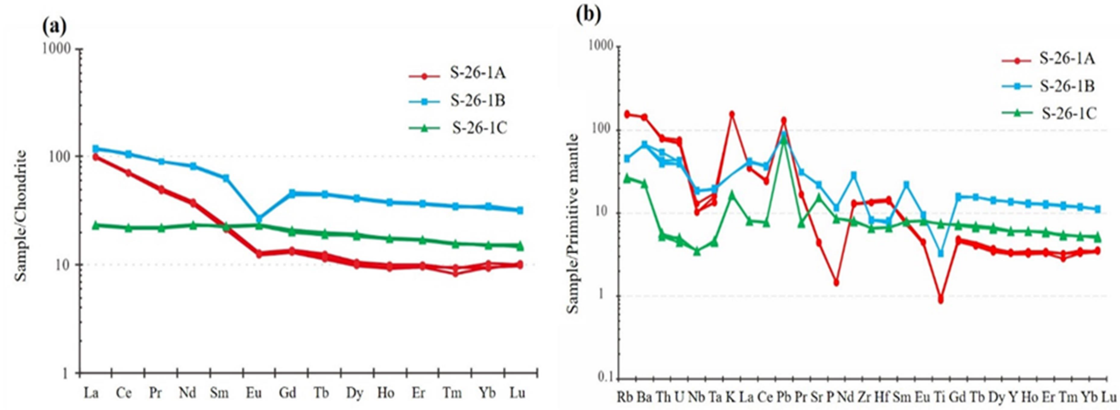

Figure 8: Diagrams REE and trace elements of the studied rocks from Tachileik area, Eastern Shan State. (a) Chondrite normalized REEs; (b) primitive mantle normalized trace elements distribution patterns. Chondrite and primitive mantle-normalized data are taken from Sun and McDonough (1989)

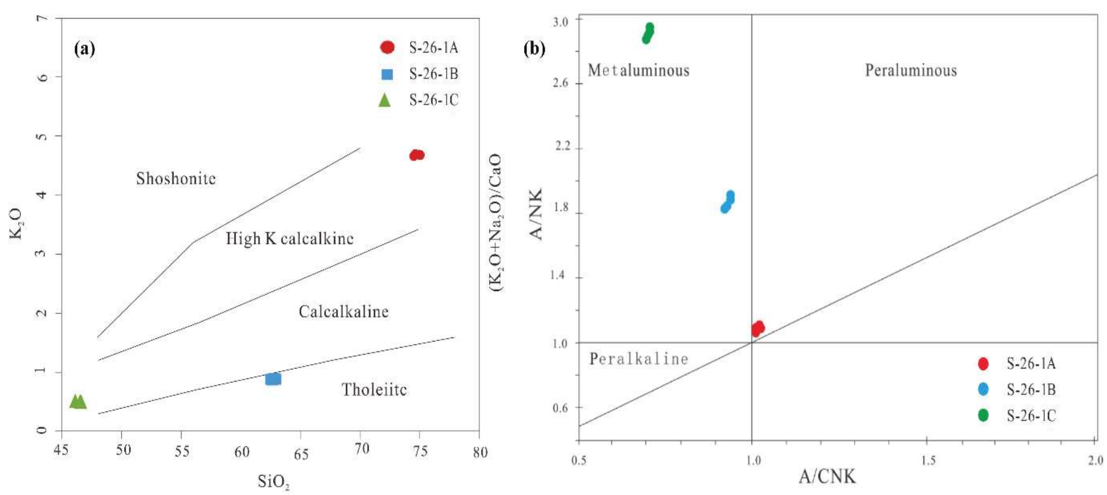

Figure 9: Classification of the plutonic rocks from the Tachileik area, Eastern Shan State. (a) SiO_2–K_2O diagram (Rickwood, 1989). (b) A/CNK–A/NK diagram (Manilar and Piccoli, 1989). (A/NK=molar ratio of $Al_2O_3/[K_2O + Na_2O]$; A/CNK=molar ratio of $Al_2O_3/[CaO + K_2O + Na_2O]$

5. Discussion

The Tachileik I-type granite (S-26/1A) exhibits high SiO_2 and Al_2O_3, and low MgO and Cr contents, along with uniform positive zircon Hf isotopic values, indicative of derivation from a single juvenile mafic continental crust. These granites display very low Sr/Y (6.1-6.3) and $(La/Yb)_N$ (9.9-10.7) values, enriched LILE and LREE, and depleted HFSE (Nb, Ta, and Ti), resembling typical modern subduction-related rocks (Pearce et al., 1984). Additionally, they fall within the volcanic arc granite field in the Nb-Y diagram and Rb/10-Hf-Ta*3(Fig. 10).

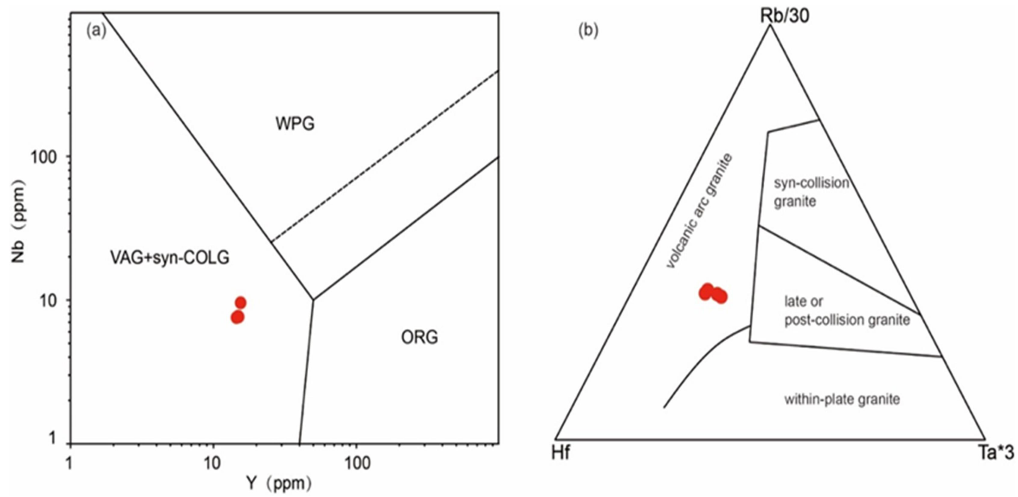

Figure 10. (a) Y-Nb discrimination diagram (Pearce, 1984) and (b) Hf-Rb/30-Ta*3 discrimination diagram (Harris et.al., 1986) for Tachileik granite tectonic setting. WPG= within plate granite; VAG= volcanic arc granite; Syn-COLG=Syn-collision granite; ORG= ocean-ridge granites.

The diorite (S-26/1B) and gabbro (S-26/1C) specimens exhibit comparable $\varepsilon_{Hf(t)}$ values ranging from +4.7 to +7.1 and +4.9 to +7, respectively. Their positive $\varepsilon_{Hf(t)}$ values, coupled with high Mg# (45-57), indicate a shared origin from depleted mantle sources. Such sources may have resulted from prior melt extraction in the mantle wedge (Cai et al., 2019). Plotting above the MORB-OIB array in the Ta/Yb-Ce/Yb diagram (Fig. 11a) indicates that their mantle source underwent modification by subduction-related components (Pearce, 1982). In Fig. 11b, the alignment of Tachileik diorite S-26/1B and gabbro S-26/1C with the sediment-derived melt trend suggests metasomatism by sediment-derived melt in their mantle sources. Additionally, the diorite and gabbro reveal flat Chondrite-normalized HREE patterns (Fig. 8a), indicating formation at relatively shallower mantle S(Ji et al., 2018). Examining the Dy/Yb vs. Gd/Yb diagram (Fig. 12, Walter, 1998) places the Tachileik diorite and gabbro within the region around the melting trend, suggesting a partial melting degree of approximately 5%-10% of upper mantle sources within the spinel stability field.

Furthermore, both diorite (S-26/1B) and gabbro (S-26/1C) present consistent REE and primitive mantle normalized trace-element patterns (Fig. 8b), resembling subduction-related rocks characterized by enrichment in large ion lithophile elements (LILEs) like Th, U, and Pb, and depletion in high field strength elements (HFSEs) such as Nb, Ta, and Ti (White and Patchett, 1984) (Fig. 8b). The Ti/Y-TZr/Y diagram (Fig.13a) indicates their formation in a plate margin setting. Moreover, in the Y/15-La/10-Nb/8 diagram (Fig.13b), the samples align with the volcanic arc basalts region, hinting at the involvement of subducted oceanic crust beneath the Indochina Block.

In summary, it is proposed that the mafic-intermediate intrusions from the earliest Carboniferous period were likely derived through the partial melting of subduction-metasomatized lithospheric mantle within the spinel stability field.

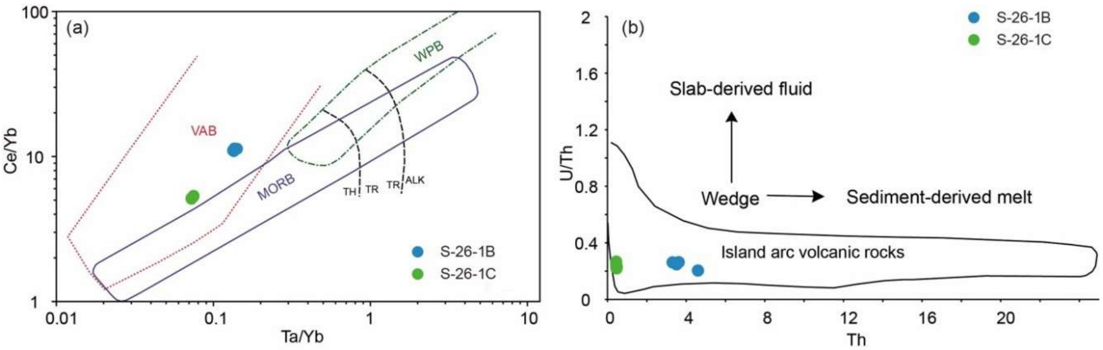

Fig.11. (a) Plots of Th/Yb vs. Ce/Yb (after Pearce, 1982). (b) Plots of Th vs. U/Th. WPB. within plate basalts; MORB. mid-ocean ridge basalts VAG. volcanic arc basalts

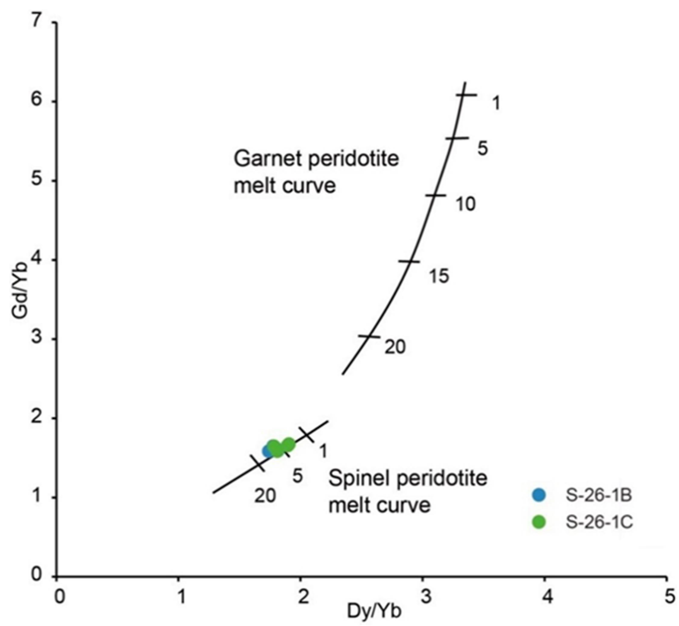

Fig. 12. Non-modal batch melting model for Gd/Yb vs. Dy/Yb (Walter, 1998). Ticks along the curves indicate the degree of melting in percent

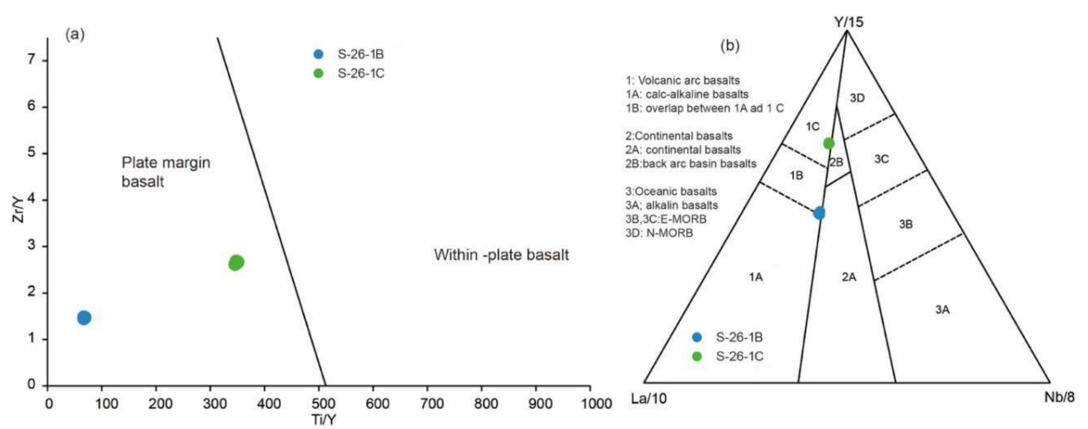

Fig. 13. (a) Zr/Y-Ti/Y discrimination diagram (after Pearce and Gale, 1977); (b) Y/15-La/10-Nb/8 diagram (after Cabanis, & Lecolle, 1989)

The Paleo-Tethys comprising the Changning-Menglian Ocean and Chiang Mai Ocean, began its formation during the Devonian (Liu et al., 1993; Fang et al., 1994; Fang and Feng, 1996; Zhong, 1998; Jian et al., 2009; Henning et al., 2009; Wang et al., 2016, 2018; Zhao et al., 2017), while collisional orogenesis commenced in the Late Triassic (Dong et al., 2013; Peng et al., 2013; Deng et al., 2018). Previous researchers have focused on unraveling the tectonic framework of the Eastern Shan State, particularly east of the Salween/Thanlwin River, and have proposed correlations with the Chiang Mai and Changning-Meglian belts in Thailand and Yunnan.

Gardiner et al. (2016) documented a zircon U-Pb age of 266 Ma with a negative Hf isotope value of -9.6±1.0 Ma on a biotite granite from north of Tachileik, near the western boundary of the Permian Sukhothai-Jinggu magmatic arc belt, suggesting it is an evolved I-type granite linked to the Sukhothai-Jinggu magmatic arc belt, formed from eastward subduction of Paleo-Tethys beneath the western margin of the Indochina Block. The closure of Paleo-Tethys, likely occurring from the Late Permian to Late Triassic, resulted in the collision of the Sibumasu block with Indochina, giving rise to Main Range and Eastern Province granites in eastern Myanmar (Gardiner et al., 2016; Metcalfe, 2013; Sone and Metcalfe, 2008; Cong et al., 2021). Hence, the Main Range and Eastern Province granitoids with Permian–Triassic ages are generally attributed to the subduction and closure of Paleo-Tethys (Searle et al., 2012; Dong et al., 2013; Peng et al., 2013; Gardiner et al., 2016; Wang et al., 2017; Deng et al., 2018; Cong et al., 2020; Liu et al., 2020).

Recently, Hu et al. (2020,2022) identified ~340 Ma Tachileik basalt formed by the partial melting of a relatively enriched mantle in the Eastern Shan State. These mafic rocks in the northern Tachileik area exhibit typical arc-like geochemical features, suggesting the initiation of the Sukhothai Arc from at least the Early Carboniferous in the Eastern Shan State.The petrological analysis of plutonic rocks from the study area near Tachileik in the Eastern Shan State reveals a range of compositions from acid to intermediate-mafic rocks, including granite, diorite, and amphibole gabbro. New zircon U-Pb dating indicates emplacement ages of 353.1-354.9 Ma, within the earliest Carboniferous.

The tectonic evolution of the Proto- and Paleo-Tethyan oceans has played an important role in determining the assembly of blocks within Gondwana and the Pangea Supercontinent in Southwest China and Southeast Asia (Li et al., 2018; Zhao et al., 2018). The Eastern Shan State serves as a crucial tectonic region linking Southwest China and Northwest Thailand, exhibiting a complex tectonic evolution from the Cambrian to the Triassic, closely associated with the Proto-Tethys and Paleo-Tethys oceans (Liu et al., 2002; Li et al., 2018; Liu et al., 2021). However, the absence of Tethyan evolution records in eastern Myanmar presents a significant challenge to comparative analysis, highlighting the necessity for investigations in this region.

Recent studies have identified two Tethyan suture belts in Southwest Yunnan, represented by the Proto-Tethyan belt and the Paleo-Tethyan belt (Liu et al., 1991; Zhong, 1998). The Changning-Menglian Suture Belt, representing the primary oceanic basin of the Paleo-Tethys in Southwest China, underwent opening in the Late Devonian, followed by subduction and closure during the Late Carboniferous to Triassic (Liu et al., 1991, 1993; Fang et al., 1994; Fang and Feng, 1996; Zhong, 1998; Wang et al., 2018). Clastic rocks of the Upper Devonian and Lower Carboniferous in this region indicate typical passive continental margin deposits on the east side of the Changning-Menglian Paleo-Tethyan Ocean, with active continental margin deposits emerging in the Upper Carboniferous, signifying eastward subduction of the oceanic crust beneath the Simao block (Liu et al., 1991, 1993; Fang et al., 1994; Fang and Feng, 1996; Zhong, 1998). The Proto-Tethyan suture belt, known as the Yunxian-Menghai Belt, comprises remnants of the Proto-Tethyan orogenic belt transformed and destroyed by the Paleo-Tethyan orogeny (Liu et al., 2021). Silurian to Early Carboniferous volcanic arcs associated with the subduction of the Proto-Tethyan Ocean crust extend into Southwest Yunnan and Tibet (Feng et al., 2000; Mao et al., 2012; Lehmann et al., 2013; Nie et al., 2016; Wei et al., 2021; Xie et al., 2021).

Recent data also suggest the presence of a subduction-related magmatic arc in the Early Carboniferous near Tachileik in the Eastern Shan State, potentially extending into more northerly areas, including Tibet (Shi et al., 2009; Hu et al., 2013). Thus, the Silurian to Early Carboniferous volcanic arc zone of the Proto-Tethys likely extended to the Tachileik region, east of the Keng Tung Granite, with further investigation required to confirm its continuation southward to Thailand.

6. Conclusions

The present investigation yields:

1) The granite samples from the Tachileik area in Eastern Myanmar exhibit zircon U-Pb ages of 353 Ma and 354 Ma, while the gabbro and diorite samples yield LA-ICP-MS zircon U-Pb dating ages of 353 Ma and 355 Ma, respectively. Early Carboniferous magmatic rocks are firstly reported in the eastern Shan State, Myanmar.
2) Analysis of geochemical and Lu-Hf isotopic data suggests that these rocks were emplaced within a subduction-related arc setting. Furthermore, they may potentially correlate with the Silurian to Early Carboniferous volcanic arc zone observed in Southwest Yunnan.
3) The Early Carboniferous subduction-related magmatic arc in the eastern Shan State, Myanmar, is attributed to the eastward subduction of the Proto-Tethys. Consequently, the presence of the Proto-Tethyan magmatic arc alongside the Paleo-Tethyan volcanic island arc is evident in the Tachileik area.

Acknowledgements

This study was financially supported by projects from the Natural Science Foundation of China (41672222). This contributes to the State Key Laboratory of Geological Process and Mineral Resources, China University of Geosciences, Wuhan. We extend our gratitude to Dr. Thet Tin Nyunt, Director General, and U Aung Kyaw Moe, Director, of the Department of Geological Survey and Mineral Exploration (DGSE), for their invaluable comments, which significantly enhanced the quality of our manuscript. Special thanks are also due to the Myanmar Federation of Mining Association (MFMA) for their generous support and assistance during the entirety of the fieldwork.

REFERENCES

Aung Min, Zaw Htet, Lwin Ko Htike, Phyoe Zaw Thwin, Si Thu Ko Ko, Kyaw Thu Aung, Phyoe Wai Win, Min Thi Ha, 2016. Local Geological Mapping and Scrutiny Report in Tarlay Sub-Township and Keng Lap Sub-Township, Tachileik Township, Shan State (East) along Myanmar-Thailand-Laos Border. pp. 1-35 (in Burmese, Unpublished).

Barber, A.J., Khin Zaw., Crow, M.J.(Eds)., 2017. The pre-Cenozoic tectonic evolution of Myanmar. In: Myanmar: Geology, Resources and Tectonics. Geological Society, London, Memoirs, 48,687-712.

Blichert-Toft, J., Chauvel, C., Albare`de, F., 1997. Separation of Hf and Lu for high-precision isotope analysis of rock samples by magnetic sector-multiple collector ICP-MS. Contributions to Mineralogy and Petrology, 127, 248-260.

Cai, H., Yang, H., & Gong, X., 2019. Geochronology and Petrogenesis of Mafic-Intermediate Intrusions on the Northern Margin of the Central Tianshan (NW China): Implications for Tectonic Evolution. Journal of Earth Science, 30(2): 323-334.

Cabanis, B. and Lecolle, M., 1989. Le diagramme La/10-Y/15-Nb/8: Un outil pour la discrimination des series volcaniques et lamise en evidence des processus demelange et/ou de contamination crustale. Compte Rendus de I'Académie des Sciences Series II, 309, 2023-2029

Cong, F., Wu, F.Y., Li, W.C., Mou, C.L., Huang, X.M., Wang, B.D., Hu, F.Y., Peng, Z.M., 2020. Origin of the Triassic Lincang Granites in the Southeastern Tibetan Plateau: Crystallization from crystal mush. Lithos, 360-361: 105452 https://doi.org/10.1016/j.lithos.2020.105452.

Cong. F., Wu, F.Y., Li, W.C., Wang, J.G., Hu, F.Y., He, D.F., Ji, W.Q., Lin, W., Kyaing Sein., (2021). Petrogenesis of the Main Range and Eastern Province granites in eastern Myanmar: New insights from zircon U-Pb ages and Sr-Nd isotopes. Lithos, 382-383: 105895.

Deng, J., Wang, C.M., Zi, J.W., Xia, R., Li, Q., 2018. Constraining subduction-collision processes of the Paleo-Tethys along the Changning-Menglian Suture: New zircon U-Pb ages and Sr-Nd-Pb-Hf-O isotopes of the Lincang Batholith. Gondw. Res., 62, 75-92.

Dilek, Y., Furnes, H., Shallo, M., 2008. Geochemistry of the Jurassic Mirdita Ophiolite (Albania) and the MORB to SSZ evolution of a marginal basin oceanic crust. Lithos, 100: 174–209.

Dong, G.C., Mo, X.X., Zhao, Z.D., Zhu, D.C., Goodman, R.C., Kong, H.L., Wang, S., 2013. Zircon U-Pb dating and the petrological and geochemical constraints on Lincang granite in Western Yunnan, China: Implications for the closure of the Paleo-Tethys Ocean. J. Asian Earth Sci., 62, 282-294.

Fang, N., Liu, B., Feng, Q., Jia, J., 1994. Late Palaeozoic and Triassic deep-water deposits and tectonic evolution of the Palaeotethys in the Changning-Menglian and Lancangjiang belts, southwestern Yunnan. Journal of Southeast Asian Earth Sciences, 9, 363-374.

Fang, N.Q., Feng, Q.L., 1996. Devonian to Triassic Tethys in Western Yunnan, China. China University of Geosciences Press, Beijing, pp. 1-135.

Feng, Q. L., Zhang, Z., Liu, B. P., et al., 2000. Radiolarian Fauna from the Longdonghe Formation at the Western Margin of the Simao Massif and Its Geologoical Significance, Journal of stratigraphy, 24(2): 126-128 (in Chinese with English abstract).

Feng, Q.L., 2002. Stratigraphy of volcanic rocks in the Changning-Menglian Belt in southwestern Yunnan. China. J. Asian Earth Sci. 20 (6), 657-664.

Gardiner, N.J., Searle M.P., Morley, C.K., Whitehouse, M.P. Whitehouse, Spencer. C.J., Robb, L.J., 2016. The Closure of Palaeo-Tethys in Eastern Myanmar and Northern Thailand: New insights from Zircon U-Pb and Hf isotope data. Gondwana Research, 39, 401-422. http://dx.doi.org/10.1016/j.gr.2015. 03.001.

Griffin, W., Pearson, N., Belousova, E., Jackson, S., Van Achterbergh, E., O'Reilly, S.Y., Shee, S., 2000. The Hf isotope composition of cratonic mantle: LAM–MC–ICPMS analysis of zircon megacrysts in kimberlites. Geochimica et Cosmochimica Acta, 64, 133–147.

Harris, N.B.W., Pearce, J.A., Tindle, A.G., 1986. Geochemical characteristics of collision-zone magmatism. In: Coward, M.P., Rles, A.C.(Eds.), Collision Tectonic. Geological Society, London, Special Publications, 19, 67-81.

Hennig, D., Lehmann, B., Frei, D., Belyatsky, B., Zhao, X.F., Cabral, A.R., Zeng, P.S., Zhou, M.F., Schmidt, K., 2009. Early Permian seafloor to continental arc magmatism in the eastern Paleo-Tethys: U-Pb age and Nd-Sr isotope data from the southern Lancangjiang zone, Yunnan, China. Lithos, 113, 408-422.

Hou, Z.Q., Gao, Y.F., Qu, X.M., Rui, Z.Y., Mo, X.X., 2004. Origin of the adakitic intrusives generated during Mid-Miocene east–west extension in southern Tibet. Earth Planet. Sci. Lett., 220, 139–155

Hu, F.Y., Wu, F.Y., Wang, J.G., 2020. The subduction of Paleo-Tethys along a continental arc in Eastern Myanmar from Carboniferous to Triassic: New insights from zircon U-Pb and Hf isotope data. Geomyanmar 2020 international congress Plus IGCP 668 & IGCP 679. January 7-8, Yangon, 38. Abs.

Hu, F.Y., Wu, F.Y., Wang, J.G., Ducea, M.N., Chapman, J.B., Zaw, K., Lin, W., Sein, K., Meffre, S., 2022. Newly discovered Early Carboniferous and Late Permian magmatic rocks in eastern Myanmar: Implications for the tectonic evolution of the eastern Paleo-Tethys. Journal of Asian Earth Sciences, 227: 105093.

Hu, P.Y., Li, C., Xie, C.M., Wu, Y.W., Wang, M., Su, L., 2013. Albite granites in Taoxinghu ophiolite in central Qiangtang, Qinghai-Tibet Plateau, China: Evidences of Paleo-Tethys oceanic crust subduction. Acta Petrologica Sinica, 29 (12): 4404-4414(in Chinese with English abstract).

Hu, Z.C., Liu, Y.S., Gao, S., Liu, W., Yang, L., Zhang, W., Tong, X., Lin, L., Zong, K.Q., Li, M., Chen, H., Zhou, L., 2012. Improved in situ Hf isotope ratio analysis of zircon using newly designed X skimmer cone and Jet sample cone in combination with the addition of nitrogen by laser ablation multiple collector ICP-MS, Journal of Analytical Atomic Spectrometry, 27, 1391-1399.

Ji, Z., Ge, W. C., Yang, H., Tian, D. X., Chen, H. J., & Zhang, Y. L., 2018. Late Carboniferous-Early Permian high-and low-Sr/Y granitoids of the Xing'an Block, northeastern China: Implications for the late Paleozoic tectonic evolution of the eastern Central Asian Orogenic Belt. Lithos, 322, 179-196.

Jian, P., Liu, D.Y., Kröner, A., Zhang, Q., Wang, Y.Z., Sun, X.M., Zhang, W., 2009. Devonian to Permian plate tectonic cycle of the Paleo-Tethys Orogen in Southwest China (I): Geochemistry of ophiolites, arc/back-arc assemblages and within-plate igneous rocks. Lithos, 113, 748-766.

Jiang, Q.Y., Li, C., Xie, C.M., Wang, M., Hu, P.Y., Wu, H., Peng, H., Chen, J.W.,2014. Geochemistry and LA-ICP-MS zircon U-Pb age of volcanic rocks of Wangguoshan Formation in the Gangmar Co area of Qiangtang, Tibet (in Chinese with English abstract). Geological Bulletin of China, 33, 1-13.

Lehmann, B., Zhao, X.F., Zhou, M.F., Du, A.D., Mao, J.W., Zeng, P.S., Henjes-Kunst, F., Heppe, K., 2013. Mid-Silurian back-arc spreading at the northeastern margin of Gondwana: The

Dapingzhang dacite-hosted massive sulfide deposit, Lancangjiang zone, southwestern China. Gondwana Research, 24, 648-663.
LeMaitre, R.W.(Ed.), 1989. A Classification of Igneous Rocks and Glossary of Terms. Blackwell Scientific Publication. Oxford, pp. 1-236.
Li, S.Z., Zhao, S.J., Liu, X., Cao, H.H., Yu, S., Li, X.Y., Lam Somerville, Yu, S.Y., Suo, Y.H., 2018. Closure of the Proto-Tethys Ocean and Early Paleozoic amalgamation of microcontinental blocks in East Asia. Earth-Science Review, 186: 37-75. https://doi.org/10.1016/j.earscirev.2017.01.011
Liu, B.P., Feng, Q.L., Fang, N.Q., 1991. Tectonic evolution of the Paleo-Tethys in Changning-Menglian and adjacent regions, western Yunnan. Journal of China University of Geoscicence, 2(1): 18-28.
Liu, B.P., Feng, Q.L., Fang, N.Q., Jia, J.H., He, F.X., 1993. Tectonic evolution of Paleo-Tethys poly-island-ocean in Changning-Menglian and Lancangjiang belts, Southwestern Yunnan, China. Earth Sci., 18, 529-538 (in Chinese with English abstract).
Liu, B.P., Feng, Q.L., Chonglakmani C., Helmcke, D., 2002. Framework of Paleo-Tethyan archipelago ocean of Western Yunnan and its elongation toward north and south. Earth Science Frontiers, 9(3): 161-171 (in Chinese with English abstract).
Liu, Y., Hu, Z., Gao, S., Gunther, D., Xu, J., Gao, C., and Chen, H., 2008. In situ analysis of major and trace elements of anhydrous minerals by LA-ICP-MS without applying an internal standard. Chem. Geol., 257: 34-43.
Liu, G.C., Sun, Z.B., Zi, J.W., M. Santosh., Zhao. T.Y., Feng, Q.L., Chen, G.Y., Nie, X.M., Li, J., Zhang, S.T., 2021. Proto-Tethys ophiolitic mélange in SW Yunnan: Constraints from zircon U-Pb geochronology and geochemistry. Geoscience Forinters., 12, 101200. https://doi.org/10.1016/j.gsf.2021.101200.
Ludwig, K.R., 2003. User's Mnual for Isoplot 3.00: A Geochronological Toolkit for Microsoft Excel. No. 4. Berkeley Geochronology Center Special Publication, Berkeley. pp. 1-70.
Manilar, P.D. and Piccoli, P.M., 1989. Tectonic discrimination of granitoids, Geol. Soc. Am. Bull., 101, 635-643.
Mao, X.C., Wang, L.Q., Bing, L.I., Wang, B. Di, Wang, D.B., 2012. Discovery of the Late Silurian volcanic rocks in the Dazhonghe area, Yunxian-Jinggu volcanic arc belt, western Yunnan, China and its geological significance, Acta Petologica Sinica, 28, 1517-1528 (in Chinese).
McBirney, A.R., 2007. Igneous Petrology. 3rd ed. Boston: Jones and Bartlett Publishers. 550.
Metcalfe, I., 1984. Stratigraphy, palaeontology and palaeogeography of the Carboniferous of Southeast Asia. Mem. Soc. Geol. France, 147, 107-118.
Metcalfe, I., 2011. Palaeozoic-Mesozoic History of SE Asia. In: Hall, R., Cottam, M., Wilson, M. (Eds.), The SE Asian Gateway: History and Tectonics of Australia-Asia Collision. Geological Society of London Special Publications, 355, 7-35.
Metcalfe, I., 2013. Gondwana dispersion and Asian Accretion: tectonic and palaeogeographic evolution of eastern Tethys. J. Asian Earth Sci., 66, 1-33.
Metcalfe, I., 2017. Tectonic Evolution of Sundaland. Bulletin of the Geological Society of Malaysia, 63, , 27-60.
Mitchell, A.H.G., 2018. Geological Belts, Plate Boundaries, and Mineral Deposits in Myanmar: Chapter 3: Myanmar East of Salween: The Sibumasu-Mong Yawng Arc Collision and Related Tin Mineralization, 77-96.
Nie, X.M., Feng, Q.L., Qian, X., Wang, Y.J., 2015. Magmatic record of Prototethyan evolution in SW Yunnan, China: geochemical, zircon U-Pb geochronological and Lu-Hf isotopic

evidence from the Huimin metavolcanic rocks in the southern Lancangjiang zone. Gondwana Research, 28, 757-768.
Nie, X.M., Feng, Q.L., Metcalfe, I., Baxter, A.T., Liu, G., 2016. Discovery of a Late Devonian magmatic arc in the southern Lancangjiang zone, western Yunnan: Geochemical and zircon U-Pb geochronological constraints on the evolution of Tethyan ocean basins in SW China. Journal of Asian Earth Sciences, 118, 32-50.
Ning, S., Wang, F., Xue, W., Zhou, T., 2017. Geochemistry of the Baoshan pluton in the Tongling region of the Lower Yangtze River Belt. Geochimica, 46, 397-412 (in Chinese with English abstract).
Pearce, J.A., Harris, N.B.W., Tindle, A.G., 1984.Trace Element Discrimination Diagrams for the Tectonic Interpretation of Granitic Rocks.Journal of Petrology, 25(4): 956-983.
Pearce, J. A., & Gale, G. H., 1977. Identification of ore-deposition environment from trace-element geochemistry of associated igneous host rocks. Geological Society, London, Special Publications, 7(1), 14-24.
Pearce, J.A., 1982. Trace element characteristics of lavas from destructive plate boundaries. In: Thorpe, R.S. (Ed.), Orogenic Andesites. Wiley, Chichester, U.K., pp. 528–548
Peng, T.P., Wilde, S.A., Wang, Y.J., Fan, W.M., Peng, B.X., 2013. Mid-Triassic felsic igneous rocks from the southern Lancangjiang Zone, SW China: Petrogenesis and implications for the evolution of Paleo-Tethys. Lithos., 168-169, 15-32.
Rapp, R.P., Watson, E.B., 1995. Dehydration Melting of Metabasalt at 8-32 Kbar:Implications for Continental Growth and Crust-Mantle Recycling. Journal of Petrology, 36(4):891-931.
Rickwood, P.C., 1989. Boundary lines within petrologic diagrams which use oxides of major and minor elements. Lithos, 22, 247-263.
Ridd, M.F., 2015. East flank of the Sibumasu block in NW Thailand and Myanmar and its possible northward continuation into Yunnan: a review and suggested tectono-stratigraphic interpretation. Journal of Asian Earth Sciences, 104, 160-174.
Searle, M.P., Whitehouse, M.J., Robb, L.J., Ghani, A.A., Hutchison, C.S., Sone, M., Ng, S.W.P., Roselee, M.H., Chung, S.L., Oliver, G.J.H., 2012. Tectonic evolution of the SibumasuIndochina terrane collision zone in Thailand and Malaysia: constraints from new UPb zircon chronology of SE Asian tin granitoids. Journal of the Geological Society, London, 169, 489-500.
Sengör, A. M. C., Altiner, D., Cin, A., Ustaomer, T., & Hsu, K. J., 1988. Origin and assembly of the Tethyside orogenic collapse at the expense of Gondwana Land. In Audley-Charles, M. G., Hallam, A., (Eds.), Gondwana and Tethys Geological Society of London.
Shi, J.R., Li, C., Dong, Y.S., 2009. Dating and Significance of plagiogranite from Guoganjianian mountain, Central Qiangtang, northern Tibet. Geol. Bull., 28 (9), 1236-1243 (in Chinese with English abstract).
Sone, S., Metcalfe, I., 2008. Parallel Tethyan sutures in mainland Southeast Asia: new insights for Palaeo-Tethys closure and implications for the Indosinian orogeny. Comptes Rendus Geoscience, 340, 166-179.
Song, S.G., Niu, Y.L., Su, L., Zhang, C., Zhang, L.F., 2014. Continental orogenesis from ocean subduction, continent collision/subduction, to orogen collapse, and orogen recycling: The example of the North Qaidam UHPM belt, NW China. Earth-Science Reviews, 129, 59-84.
Sun, S.S., McDonough, W.F., 1989. Chemical and isotopic systematics of oceanic basalts: implications for mantle composition and processes. Geol. Soc. Spec. Publ., 42, 313–345.
Taylor, S.R., McLennan, M.S., 1995. The geochemical evolution of the continental crust. Rev. Geophys., 33, 293–301.

Walter M.J., 1998. Melting of garnet peridotite and the origin of komatiite and depleted lithosphere. Journal of Petrology, 39, 29-60

Wang, Y.J., Qian, X., A, C.P., Liu, H.C., Feng, Q.L., Zhao, G.C., Zhang, Y.H., He, H.Y., Zhang, P.Z., 2018. Closure of the East Paleotethyan Ocean and amalgamation of the Eastern Cimmerian and Southeast Asia continental fragments. Earth-Sci. Rev., 186, 195-230.

Wang, B., Wang, L., Chen, J., Liu, H., Yin, F., Li, X., 2017. Petrogenesis of Late Devonian-Early Carboniferous volcanic rocks in northern Tibet: New constraints on the Paleozoic tectonic evolution of the Tethyan Ocean. Gondwana Research, 41, 142-156.

Wang, Y.J., He, H.Y., Cawood, P.A., Srithai, B., Feng, Q.L., Fan, W.M., Zhang, Y.Z., Qian, X., 2016. Geochronological, elemental and Sr-Nd-Hf-O isotopic constraints on the petrogenesis of the Triassic post-collisional granitic rocks in NW Thailand and its Paleotethyan implications. Lithos, 266-267, 264-286.

Wei, Y.H., Zi, J.W., Liu, G.C., Sun, Z.B., Chen, G.Y., Zhao, T.Y., Nie, X.M., Yang, Z., 2022. Reconstructing the Lancang Terrane (SW Yunnan) and implications for early Paleozoic Proto-Tethys evolution at the northern margin of Gondwana. Gondwana Research, 101: 278-294.

Wei, Y.H., Gan, Z.Q., Liu, G.C., Feng, Q.L., 2021. The Stratigraphic sequence and geological time of Dawazi Formation in western Simao Block. Earth Sci., 46(2): 418-431, doi: 10.3799/dqkx.2020.066 (in Chinese with English Abstract).

White, W.M., Patchett, P.J., 1984. Hf-Nd-Sr isotopes and incompatible element abundances in island arcs: implications for magma origins and crust-mantle evolution. Earth Planet. Sci. Lett., 67, 167-185.

Xie, S.W.， Liu, F.L., Wang, F., 2021. Petrogenesis of Late Devonian volcanic rocks in the Jinghong area， southwestern Sanjiang region and its geological implications. Acta Petrologica Sinica， 37 (2) : 481-496 (in Chinese with English abstract).

Xin, Y., Li, J., Dong, S., Zhang, Y., Wang, W., Sun, H., 2017. Neoproterozoic post-collisional extension of the central Jiangnan Orogen: Geochemical, geochronological, and Lu-Hf isotopic constraints from the ca. 820–800 Ma magmatic rocks. Precambrian Research, 294, 91-110.

Yang, W.Q., Feng, Q.L., Duan, X.D., 2007. Late Devonian pillow basalt and bedded chert in Changning-Menglian tectonic belt of southwestern Yunnan, China. Geological Bulletin of China, 26(6): 739-747.

Zhao, G.C., Wang, Y.J., Huang, B.C., Dong, Y.P., Li, S.Z., Zhang, G.W., Yu, S., 2018. Geological reconstructions of the East Asian blocks: from the breakup of Rodinia to the assembly of Pangea. Earth Sci. Rev., 186, 262-286.

Zhao, T.Y., Feng, Q.L., Metcalfe, I., Milan, L.A., Liu, G.C., Zhang, Z.B., 2017. Detrital zircon U-Pb-Hf isotopes and provenance of Late Neoproterozoic and Early Paleozoic sediments of the Simao and Baoshan blocks, SW China: Implications for Proto-Tethys and Paleo-Tethys evolution and Gondwana reconstruction. Gondwana Research, 51: 193-208.

Zhong, D.L., 1998. The Paleotethys Orogenic Belt in West of Sichuan and Yunnan. Science Publishing House, Beijing, pp. 1-231 (in Chinese).